International Journal of Polymeric Materials, 54:933–948, 2005

ISSN: 0091-4037 print/1563-5333 online
DOI: 10.1080/00914030390504717l

Taylor & Francis
Taylor & Francis Group

Rheology of Short Nylon-6 Fiber Reinforced Styrene-Butadiene Rubber

A. Seema
S. K. N. Kutty
Department of Polymer Science and Rubber Technology,
Cochin University of Science and Technology, Cochin, India

The rheological characteristics of short Nylon-6 fiber reinforced styrene butadiene rubber (SBR) were studied using a capillary rheometer. The study was done with respect to the effect of shear rate, fiber concentration, and temperature on shear viscosity and die swell. All the melts showed pseudoplastic nature, which decreased with increasing temperature. Shear viscosity increased in the presence of fibers. Introduction of fiber reduces the temperature sensitivity of the rubber matrix. A reduction in die swell was found in presence of fibers.

Keywords: styrene butadiene rubber, short Nylon-6 fiber, composite, shear stress, shear rate, shear viscosity, die swell, activation energy

INTRODUCTION

Short fibers, natural and manmade, are used as reinforcing agents in rubber to improve the processing and strength of the rubber [1–4]. One of the characteristic features of short fiber rubber composites is their combination of high strength and elasticity, which originates from the flexibility of the rubber and the reinforcing effect of the fibers [4–8]. As many processing steps in the modern rubber industry involve a flow of polymer, knowledge of the flow characteristics of the composite is essential. During processing, a rubber compound is subjected to various forms of shear such as mixing, calendaring, and extrusion. The rheological behavior of polymer melts dictates the choice of processing conditions and influences the morphology and mechanical

Received 7 May 2004; in final form 25 June 2004.
Address correspondence to S. K. N. Kutty, Department of Polymer Science and Rubber Technology, Cochin University of Science and Technology, Cochin 682 022, India. E-mail: sunil@cusat.ac.in

properties of the final product. The need for rheological studies and their importance in the selection of processing conditions were pointed out by Brydson [9]. White and Tokita established a correlation between rheology and processing [10–12]. Crowson et al. reported the rheology of short glass fiber reinforced thermoplastics and found that fibers orient along the flow direction in the convergent flow and perpendicular to the flow direction in the divergent flow [13–14]. Several studies on the reheological characteristics of short fiber reinforced polymer melts have been reported [15–19]. Murty et al. studied the rheology of short jute fiber filled natural rubber composites [20]. Many studies were done to evaluate the dependence of the die swell on the L/D(length to diameter) ratio of the capillary [21–23]. Kutty et al. reported the rheological characteristics of short Kevlar fiber reinforced thermoplastic polyurethane [24]. Rheological behavior or short sisal fiber reinforced natural rubber composite was studied by Vargehse et al. [25]. Rheological properties of short polyester fiber polyurethane elastomer composite with and without bonding agent were reported by Suhara et al. [26–27]. The present work deals with the rheological characteristics of short Nylon-6 fiber reinforced styrene butadiene rubber with respect to the effect of shear rate, fiber concentration, and temperature on shear viscosity and die swell.

EXPERIMENTAL

Materials

Styrene butadiene rubber (synaprene 1502) was obtained from Synthetics and Chemicals Ltd., Bareilly. Nylon-6 fiber of diameter 20 μm obtained from SRF Ltd., Madras, was chopped to approximately 6 mm length. Zinc oxide (ZnO) was obtained from M/s Meta Zinc Ltd., Bombay. Stearic acid was procured from Godrej Soap (Pvt.) Ltd., Bombay, India.

Processing

Formulation of mixes is given in Table 1. These mixes were prepared as per ASTM D 3182 (1989) on a laboratory size two roll mixing mill. The compounding temperature was kept below 90°C by passing water through the mill rolls.

Rheological studies were carried out using a capillary rheometer attached to a Shimadzu Universal Testing Machine Model AG-I 50KN. A capillary of L/D 10 and an angle of entry 90° was used. The measurements were carried out at various shear rates ranging from

TABLE 1 Composition of Mixes (Parts by Weight)

Mix	A	B	C	D
SBR	100	100	100	100
Nylon	0	10	20	30
ZnO	5	5	5	5
Stearic acid	1.5	1.5	1.5	1.5

$1.6\,s^{-1}$ to $831.2\,s^{-1}$. The temperature difference between different zones was kept to a minimum. Small strips of composites were placed inside the barrel and warmed for a minute. Then they were forced down with a plunger attached to the moving cross-head. The height of the melt in the barrel before extrusion was kept constant in all runs. The experiments were carried out at six different shear rates obtained by moving the cross-head at preselected speeds (1 to 500 mm/min). The force corresponding to different plunger speeds was recorded. The true shear stress was calculated as [9]

$$\tau_w = \frac{PR}{2L}$$

where τ_w is the shear stress at the wall, P is the pressure drop, L is the length of the capillary, and R is the radius of the capillary.

Apparent shear rate, shear rate at wall and viscosity were calculated using the following equations [9]

$$\gamma_a = \frac{32Q}{\pi d_c^3}$$

$$\gamma_w = \frac{(3n+1)\gamma_a}{4n}$$

$$\eta' = \frac{\tau_w}{\gamma_w}$$

where: γ_a is the apparent shear rate (s^{-1}); Q is the volumetric flow rate ($mm^3 s^{-1}$); d_c is the diameter of the capillary (mm), γ_w is the shear rate at wall (s^{-1}); n′ is the flow behavior index, and η is the shear viscosity (Pa.s).

n′ was calculated by the liner regression from log (τ_w) and log (γ_a). The extrudates emerging from the capillary were collected with the utmost care to avoid any further deformation and the diameters were measured after a relaxation period of 24 h. The die swell was calculated as the ratio of the diameter of the extrudate to that of the

capillary (d_e/d_c). The relaxed extrudates were cut across the length using a sharp razor; the fresh surfaces were gold sputtered and examined under SEM.

RESULTS AND DISCUSSIONS

Effect of Shear Rate on Shear Viscosity

Figures 1–3 show the variation of viscosity with shear rate of all the mixes at 80, 90, and 100°C, respectively. In all the cases it is seen that the viscosity decreases almost linearly with shear rate in the shear rate range studied, indicating a pseudoplastic behavior of the composite. The reduction in viscosity with increasing shear rate may arise from the molecular alignment during flow through the capillary. The fact that the pattern is also observed in the case of fiber filled mixes indicates that the fibers, while restricting the free flow of the melt, also get aligned in the direction of flow. This is evident from SEM photomicrograph of extrudates of mix D. Figures 4a and 4b show the SEM photomocrograph of cut surfaces of extrudates of mix D at shear rates $1\,s^{-1}$ and $100\,s^{-1}$, respectively at 100°C. Higher level of orientation at higher shear rate is evident from Figure 4b. The cut

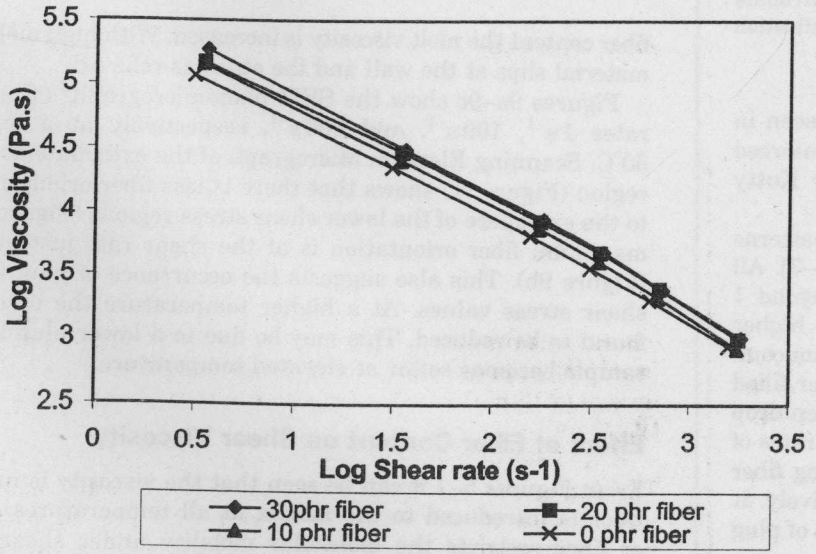

FIGURE 1 Shear viscosity versus shear rate at 80°C.

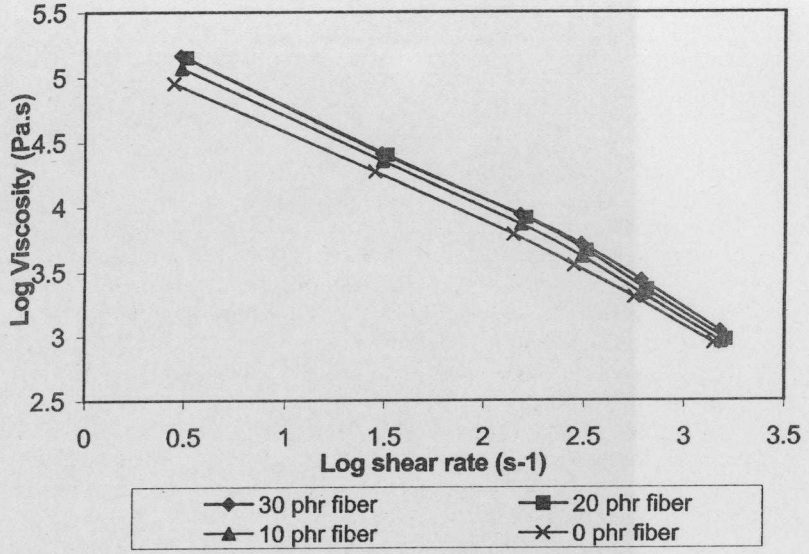

FIGURE 2 Shear viscosity versus shear rate at 90°C.

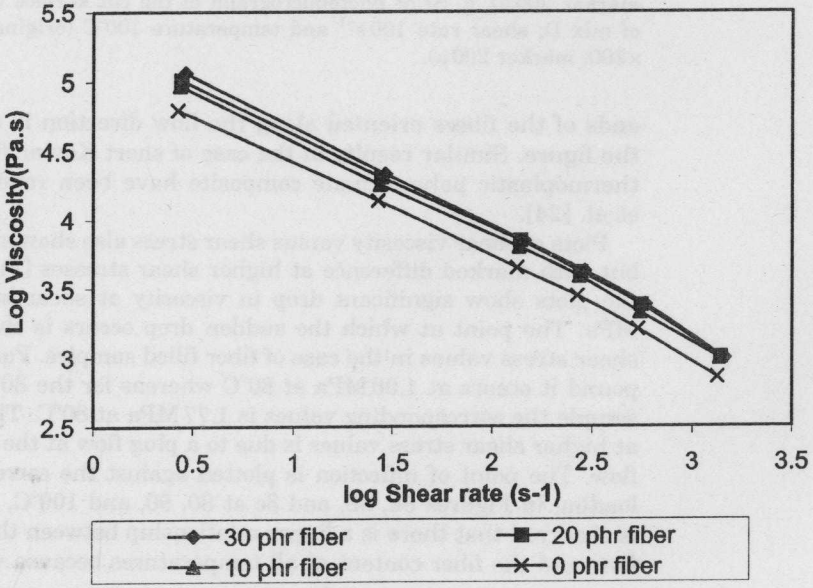

FIGURE 3 Shear viscosity versus shear rate at 100°C.

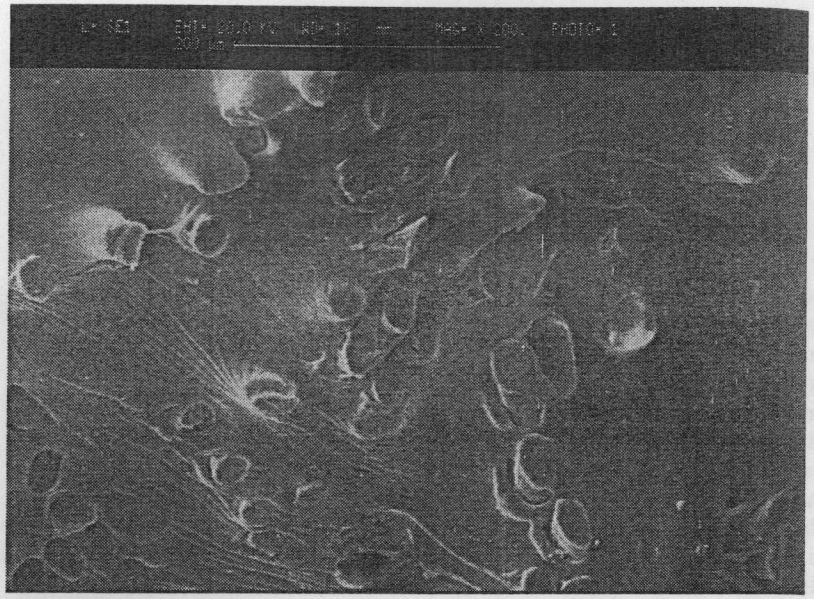

FIGURE 4 a. SEM photomicrograph of the cut surface of the extrudate of mix D; shear rate $1\,s^{-1}$ and temperature 100°C (original magnification ×200; marker 200 μ). b. SEM photomicrograph of the cut surface of the extrudate of mix D; shear rate $100\,s^{-1}$ and temperature 100°C (original magnification ×200; marker 200 μ).

ends of the fibers oriented along the flow direction is clearly seen in the figure. Similar results in the case of short Kevlar fiber reinforced thermoplastic polyurethane composite have been reported by Kutty et al. [24].

Plots of shear viscosity versus shear stress also show similar patterns but with marked difference at higher shear stresses [Figures 5–7]. All the plots show significant drop in viscosity at shear stress beyond 1 MPa. The point at which the sudden drop occurs is shifted to higher shear stress values in the case of fiber filled samples. For the gum compound it occurs at 1.08 MPa at 80°C whereas for the 30 phr fiber filled sample the corresponding values is 1.77 MPa at 80°C. The sudden drop at higher shear stress values is due to a plug flow at the higher rates of flow. The point of inflection is plotted against the corresponding fiber loading in Figures 8a, 8b, and 8c at 80, 90, and 100°C, respectively. It is observed that there is a linear relationship between the onset of plug flow and the fiber content at all temperatures because with increasing

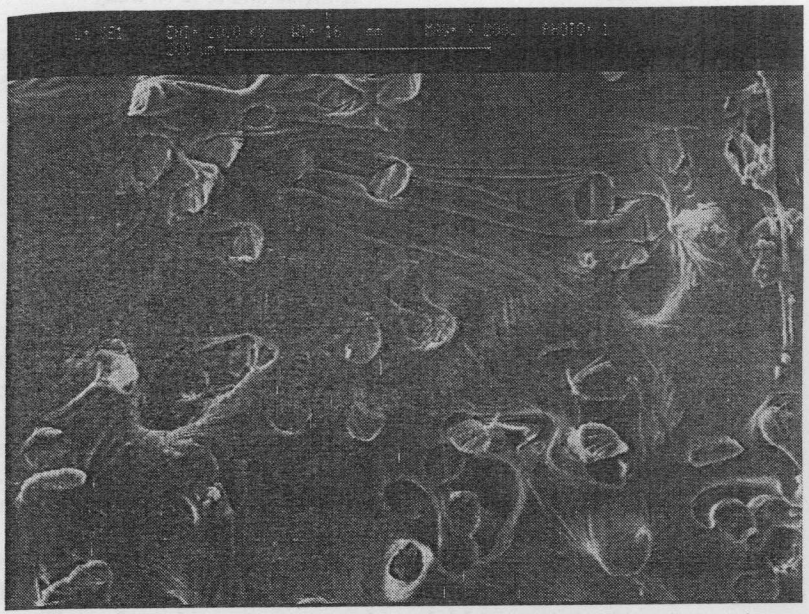

FIGURE 4 Continued.

fiber content the melt viscosity is increased. With high melt viscosity the material slips at the wall and the stress is relieved.

Figures 9a–9c show the SEM photomicrographs of mix D at shear rates $1\,s^{-1}$, $100\,s^{-1}$, and $500\,s^{-1}$, respectively at a temperature of 80°C. Scanning Electron Micrograph of the extrudate at the plug flow region (Figure 9c) shows that there is less fiber orientation compared to the extrudate of the lower shear stress regions (Figures 9a–9b). The maximum fiber orientation is at the shear rate just above the drop (Figure 9b). This also suggests the occurrence of plug flow at higher shear stress values. At a higher temperature the extent of drop is found to be reduced. This may be due to a lower plug flow when the sample becomes softer at elevated temperature.

Effect of Fiber Content on Shear Viscosity

From Figures 5–7 it can be seen that the viscosity is increased when fiber is introduced to the matrix at all temperatures. The presence of fiber restricts the molecular mobility under shear, resulting in higher viscosity. With further increase in fiber concentration there is

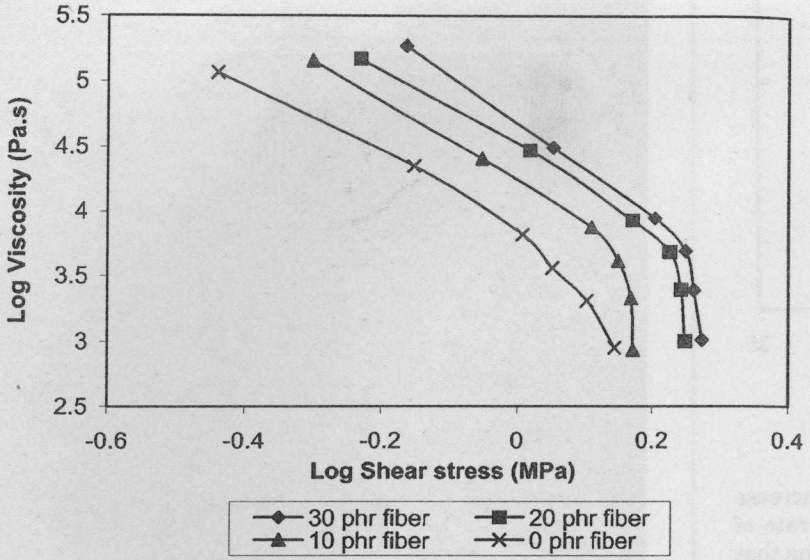

FIGURE 5 Shear viscosity versus shear stress at 80°C.

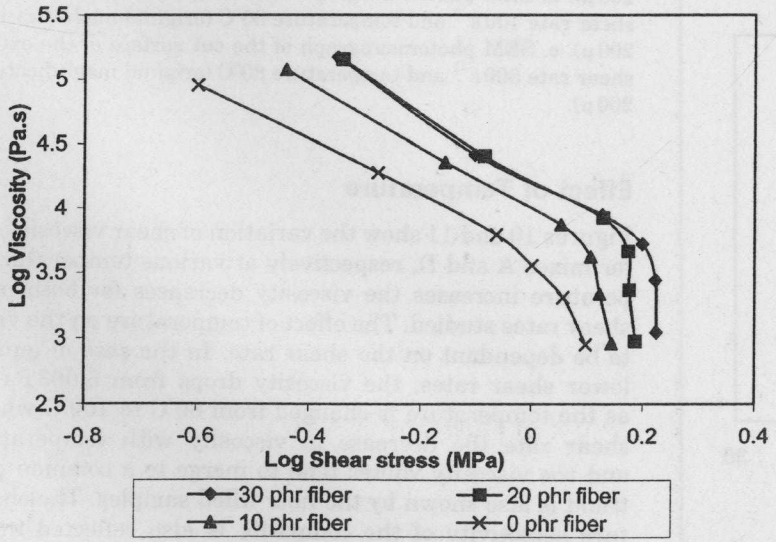

FIGURE 6 Shear viscosity versus shear stress at 90°C.

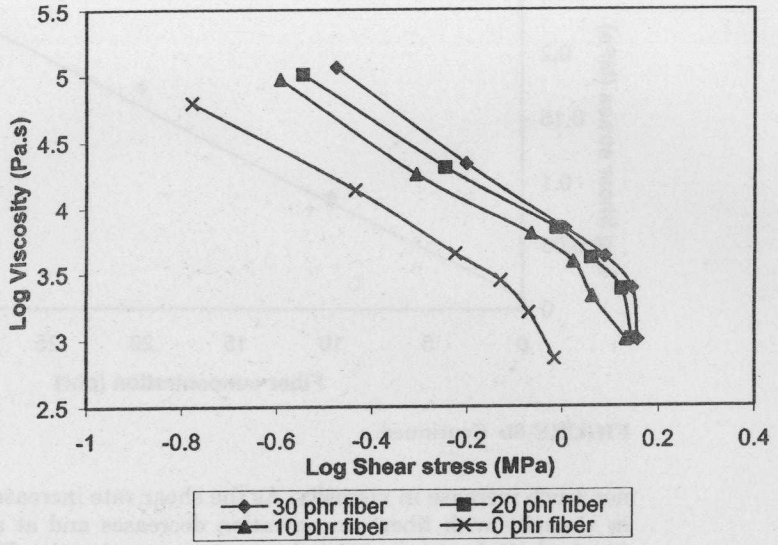

FIGURE 7 Shear viscosity versus shear stress at 100°C.

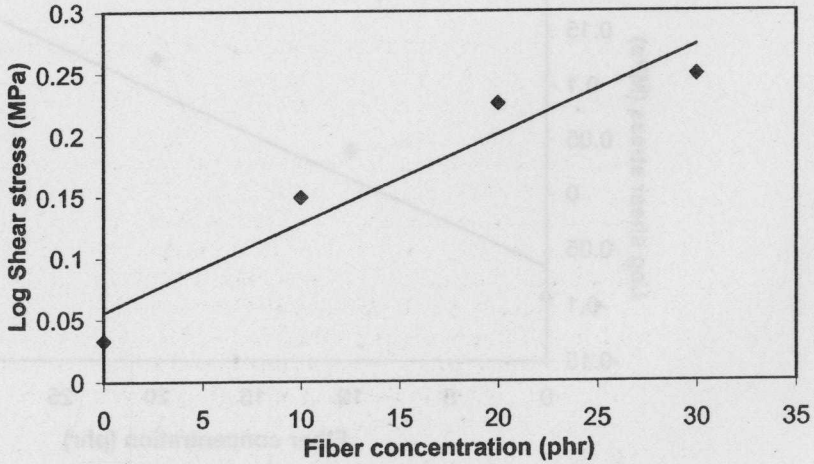

FIGURE 8 Variation of shear stress at the point of inflection with fiber loading at: a. 80°C; b. 90°C; c. 100°C.

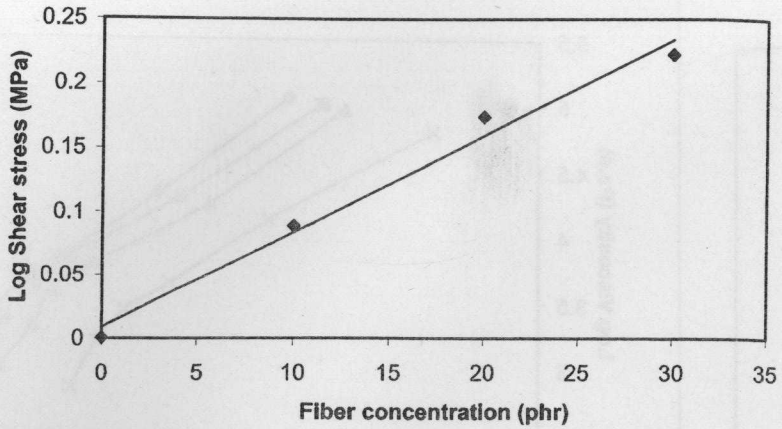

FIGURE 8b Continued.

not much increase in viscosity. As the shear rate increases, the increase in viscosity with fiber concentration decreases and at a shear rate of $831.2\,s^{-1}$ all the mixes show almost the same viscosity. This means that the effect of fiber on shear viscosity is prominent at lower shear rates only. This is in agreement with earlier observations [17,24].

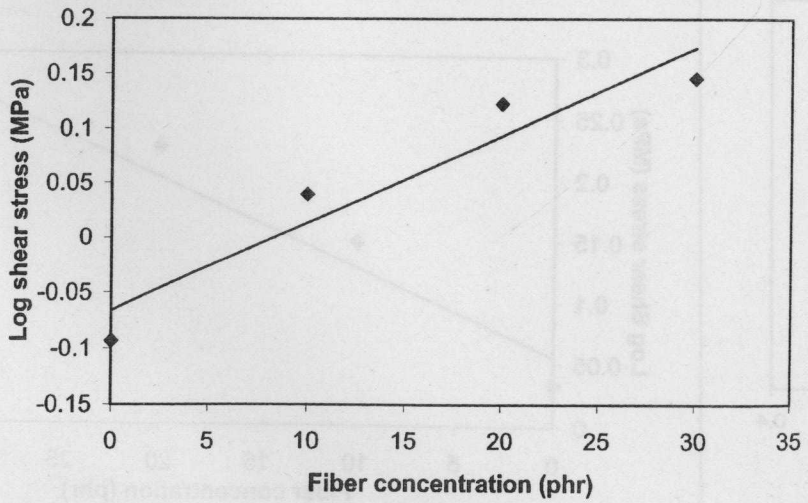

FIGURE 8c Continued.

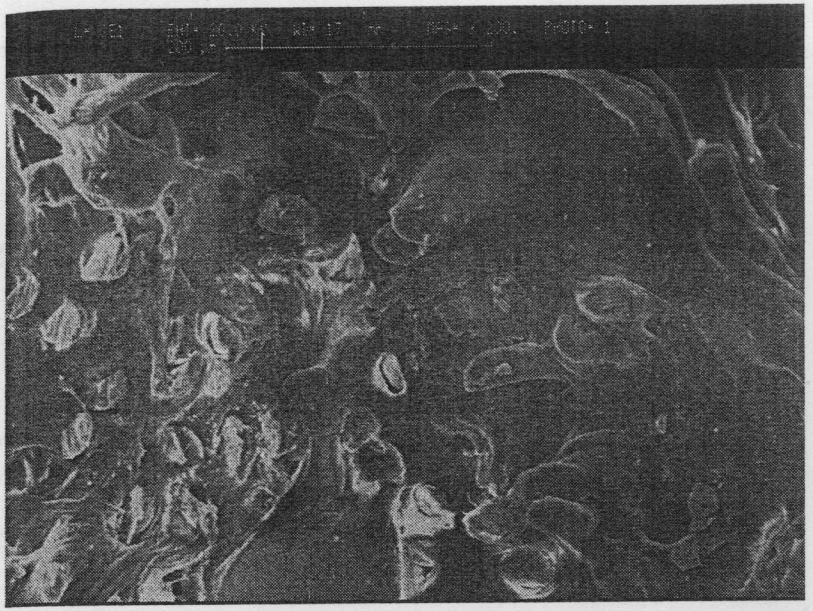

FIGURE 9 a. SEM photomicrograph of the cut surface of the extrudate of mix D; shear rate $1\,s^{-1}$ and temperature 80°C (original magnification ×200; marker 200 μ). b. SEM photomicrograph of the cut surface of the extrudate of mix D; shear rate $100\,s^{-1}$ and temperature 80°C (original magnification ×200; marker 200 μ). c. SEM photomicrograph of the cut surface of the extrudate of mix D; shear rate $500\,s^{-1}$ and temperature 80°C (original magnification ×200; marker 200 μ).

Effect of Temperature

Figures 10 and 11 show the variation of shear viscosity with shear rate for mixes A and D, respectively at various temperatures. As the temperature increases the viscosity decreases for both mixes at all the shear rates studied. The effect of temperature on the viscosity is found to be dependant on the shear rate. In the case of gum compound, at lower shear rates, the viscosity drops from 5.063 Pa.s to 4.795 Pa.s as the temperature is changed from 80°C to 100°C whereas at higher shear rate the decrease in viscosity with temperature is reduced and the viscosity values tend to merge to a common point. A similar trend is also shown by the fiber filled samples. The changed temperature sensitivity of the composite is also reflected in the calculated activation energy values (Table 2).

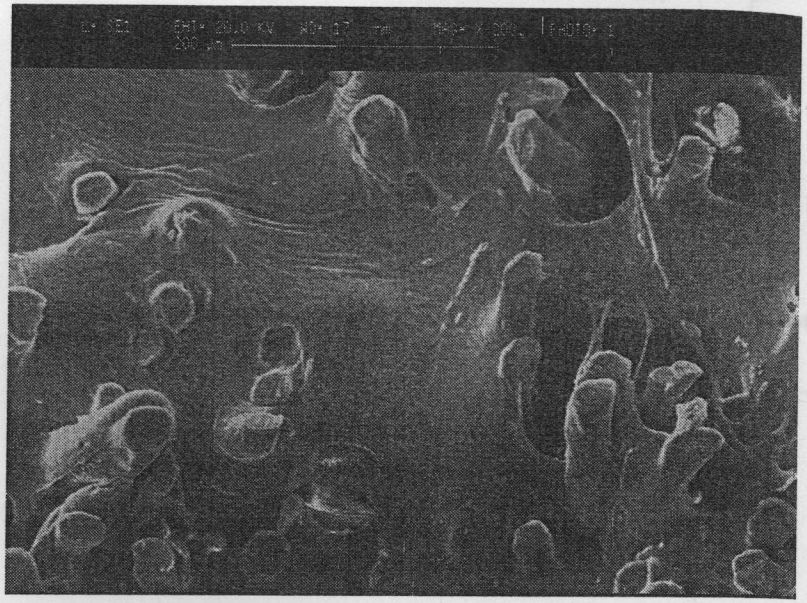

FIGURE 9b Continued.

In the case of 30 phr fiber loading (Figure 11) the log viscosity decreases from 5.27 Pa.s to 5.06 Pa.s at a lower shear rate of 1.6 s^{-1}. But as the shear rate increases, the drop in viscosity with temperature decreases more in mix D than in mix A.

Activation Energies

The activation energies of mixes A to D were calculated from the Arrhenius plots of viscosity and temperatures at different shear rates and are given in Table 2. The activation energy of flow, an indication of the temperature sensitivity of the melts, is reduced in the presence of fibers. This indicates that the higher temperature sensitivity of flow of the rubber matrix is reduced in the presence of fibers. Similar trends were reported earlier [24]. The activation energy of all the melts decreases as shear rate increases. This indicates that the temperature sensitivity of the gum and composite melts are also shear dependent and the sensitivity is lower at higher shear rates.

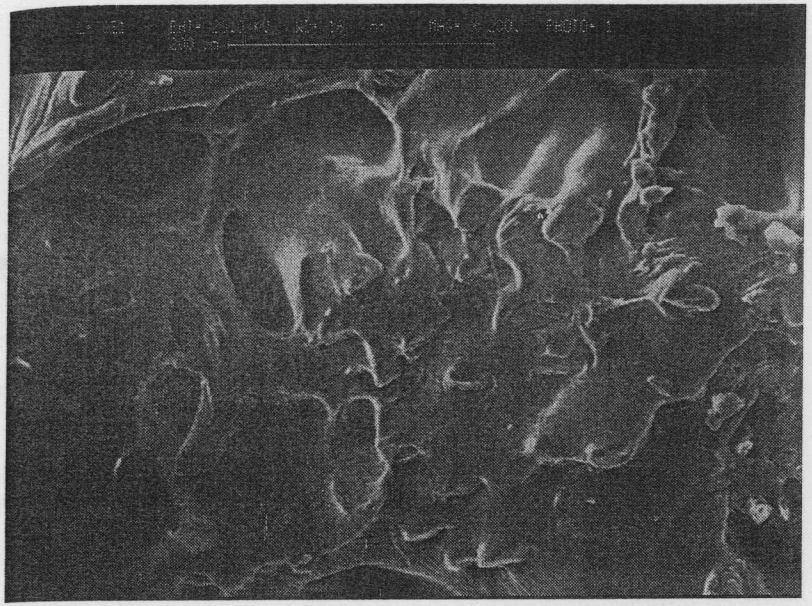

FIGURE 9c Continued.

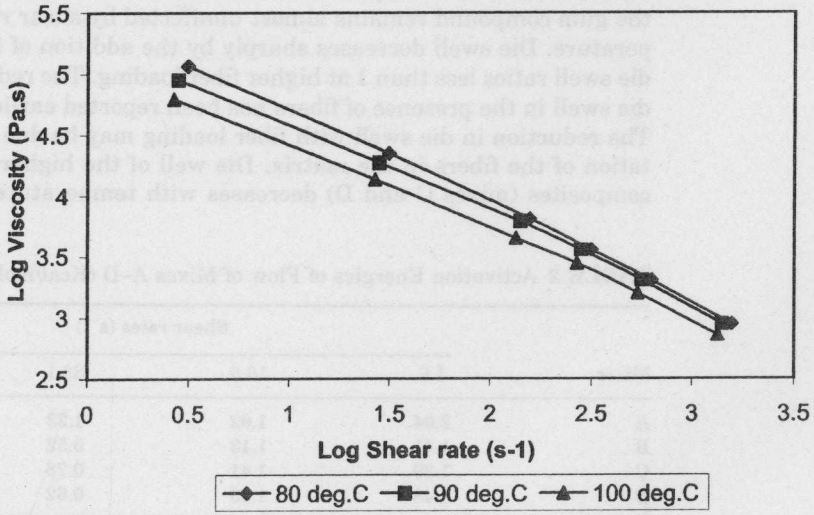

FIGURE 10 Shear viscosity versus shear rate for mix A.

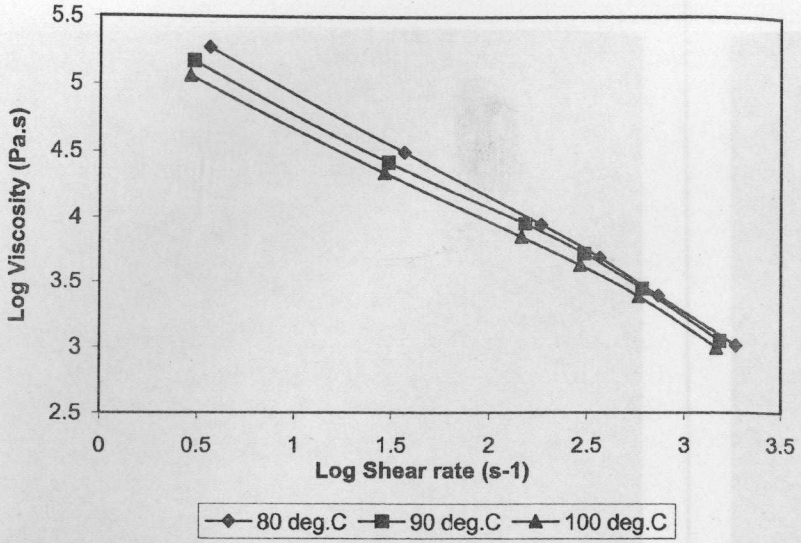

FIGURE 11 Shear viscosity versus shear rate for mix D.

Die Swell

Table 3 gives the die swell ratio (d_e/d_c) of the gum and fiber filled mixes at different temperatures and shear rates. The die swell of the gum compound remains almost unaffected by shear rate and temperature. Die swell decreases sharply by the addition of fiber and the die swell ratios less than 1 at higher fiber loading. The reduction in the die swell in the presence of fibers has been reported earlier [17,20,24]. The reduction in die swell with fiber loading may be due to the orientation of the fibers in the matrix. Die well of the higher fiber loaded composites (mixes C and D) decreases with temperatures, especially

TABLE 2 Activation Energies of Flow of Mixes A–D (Kcal/mol^{-1})

	Shear rates (s^{-1})			
Mixes	1.6	16.6	83.1	166.2
A	2.04	1.62	1.23	0.84
B	1.41	1.13	0.52	0.16
C	1.39	1.41	0.78	0.66
D	1.48	1.05	0.62	0.34

TABLE 3 Die Swell Ratios of Mixes A–D at Different Temperatures

		Shear rates (s^{-1})					
Mix	Temperature (°C)	1.6	16.6	83.1	166.2	332.5	831.2
A	80	1.28	1.22	1.22	1.22	1.62	1.76
	90	1.25	1.25	1.25	1.29	1.34	1.57
	100	—	—	1.30	1.46	1.77	1.58
B	80	1.03	1.03	1.03	1.03	1.18	1.32
	90	0.946	0.946	1.01	1.08	1.08	1.35
	100	1.14	1.22	1.52	1.39	1.48	1.13
C	80	0.972	0.972	1.06	0.972	0.972	1.065
	90	0.921	0.921	0.964	0.964	1.05	1.05
	100	0.897	0.897	1.15	1.41	1.28	1.15
D	80	0.986	0.986	0.939	0.891	0.891	0.915
	90	0.921	0.921	1.05	1.05	0.921	1.05
	100	0.812	0.875	1.08	1.21	1.08	1.00

at lower shear rates, and at higher shear rates the die swell remains more or less constant with temperature.

CONCLUSIONS

Short Nylon-6 fiber reinforced styrene butadiene rubber composites exhibit pseudoplasticity, which decreases with temperature. The shear viscosity is increased in the presence of fibers and the effect is pronounced at lower shear rates. The presence of fibers reduces the temperature sensitivity of the flow at a given shear rate. The fibers get oriented in the direction of flow at higher shear rates. There is a reduction in die swell in the presence of fibers.

REFERENCES

[1] Derringer, G. C., *Rubber world* **165**, 45 (1971).
[2] Boustany, K. and Arnold, R. L., *J. Elastoplast.* **8**, 160 (1976).
[3] Moghe, S. R., *Rubber Chem. Technol.* **47**, 1074 (1794).
[4] O' Connor, J. E., *Rubber Chem. Technol.* **50**, 945 (1977).
[5] Coran, A. Y., Boustany, K., and Hamed, P., *Rubber Chem. Technol.* **47**, 396 (1974).
[6] Coran A. Y., Boustany, K., and Hamed, P., *J. Appl. Polym. Sci.* **15**, 2471 (1975).
[7] Chakraborty, S. K., Setua, D. K., and De, S. K., *Rubber Chem. Technol.* **55**, 1286 (1982).
[8] Murty, V. M. and De, S. K., *Rubber Chem. Technol.* **55**, 287 (1982).
[9] Brydson, J. A. (1981). *Flow Properties of Polymer Melts*, 2nd ed. George Godwin, London, pp. 18–28.

[10] White, J. L., *Rubb. Chem. Technol.* **42**, 257 (1969).
[11] White, J. L., and Tokita, N., *J. Appl. Polym. Sci.* **11**, 321 (1967).
[12] White, J. L., *Rubb. Chem. Technol.* **50**, 163 (1977).
[13] Crowson, M. J., Flokes, M. J., and Bright, P. F., *Poly. Eng. Sci.* **20**, 925 (1980).
[14] Crowson, J. and Flokes, M. J., *Poly. Eng. Sci.* **20**, 934 (1980).
[15] Goettler, L. A., Lambright, A. J., Leib, R. I., and Dimauro, P., *Rubb. Chem. Technol.* **54**, 277 (1981).
[16] Goettler, L. A., Leib, R. I., and Lambright, A. J. *Rubb. Chem. Technol.* **52**, 838 (1979).
[17] Chan, Y., White, J. L., and Oyanagi, Y. *J. Rheol.* **22**, 507 (1978).
[18] Setua, D. K., *Int. J. Polym. Mater.* **11**, 67 (1985).
[19] Kuruvilla, J., Kuriakose, B., Premalatha, C. K., Thomas, S., and Pavithran, C., *Plast. Rub. Compos. Process Appl.* **21**, 237 (1994).
[20] Murty, V. M., Gupta, B. R., and De, S. K., *Plast. Rub. Proc. Appl.* **5**, 307 (1985).
[21] Arai, T., and Aoyama, H., *Trans. Soc. Rheol.* **7**, 333, (1963).
[22] Rogers, M. G., *J. Appl. Polym. Sci.* **14**, 1679 (1970).
[23] Han, C. D., Charles, M., and Philippoff, W., *Trans. Soc. Rheol.* **14**, 393 (1970).
[24] Kutty, S. K. N., De, P. P., and Nando, G. B., *Plast. Rub. Compos. Process Appl.* **15**, 23 (1991).
[25] Vargehse, S., Kuriakose, B., Thomas, S., Premalatha, C. K., and Koshy, A. T., *Plast. Rub. Compos. Process Appl.* **20**, 93 (1993).
[26] Suhara, F., Kutty, S. K. N., and Nando, G. B., *Polym. Plast. Technol. Eng.* **36**, 399 (1997).
[27] Suhara, F., Kutty, S. K. N., Nando, G. B., and Bhattacharya, A. K., *Polym. Plast. Technol. Eng.* **37**, 57 (1998).

International Journal of Polymeric Materials, 54:949–961, 2005

ISSN: 0091-4037 print/1563-5333 online
DOI: 10.1080/009140390504762

Taylor & Francis
Taylor & Francis Group

Synthesis and Structure Characterization of Boron-Nitrogen Containing Phenol Formaldehyde Resin

Jungang Gao
Xiaohui Su
Liya Xia
Department of Polymer Science, College of Chemistry and Environmental Science, Hebei University, Baoding, China

A boron-nitrogen modified phenol formaldehyde resin (BNPFR) was prepared from phenol, formalin, ammonia water, n-butyl alcohol, boric acid, and paraformaldehyde. The reaction mechanism and structure of BNPFR during the synthesis and curing process were investigated by FTIR, NMR. The thermal stability was determined by thermogravimetric analysis. The results showed that borate, ether linkage, methylene bridges, and hexatomic ring containing coordinate linkage of boron-nitrogen were formed mostly in the synthesis and thermosetting process. The carbonyl group was formed in the synthesis and curing process at higher temperature. The initial thermal degradation temperature of BNPFR is 100°C higher than common phenol formaldehyde resin (PFR).

Keywords: phenolic resin, boron-nitrogen containing, synthesis

INTRODUCTION

Phenol formaldehyde resins (PFRs) are used principally in the reinforced thermosetting materials. To improve the flame retardancy and thermo-oxidative resistance of PFR, the addition of boron has been reported [1–4]. The effectiveness of the borate as flame-retardants in various materials has been explained by their formation of nonpenetrable glass coating in these materials upon their thermal degradation. The glass coatings exclude oxygen and prevent further

Received 17 June 2004; in final form 26 June 2004.
Address correspondence to Jungang Gao, Department of Polymer Science, College of Chemistry and Environmental Science, Hebei, University, Baoding 071002, China. E-mail: gaojg@mail.hbu.edu.cn